Integrable Digital Quantum Simulation: Generalized Gibbs Ensembles and Trotter Transitions

Eric Vernier,[1] Bruno Bertini,[2,3] Giuliano Giudici,[4,5] and Lorenzo Piroli[6]

[1]*CNRS and Université Paris Cité, Laboratoire de Probabilités, Statistique et Modélisation, F-75013 Paris, France*
[2]*School of Physics and Astronomy, University of Nottingham, Nottingham, NG7 2RD, United Kingdom*
[3]*Centre for the Mathematics and Theoretical Physics of Quantum Non-Equilibrium Systems, University of Nottingham, Nottingham, NG7 2RD, United Kingdom*
[4]*Arnold Sommerfeld Center for Theoretical Physics, University of Munich, Theresienstr. 37, 80333 München, Germany*
[5]*Munich Center for Quantum Science and Technology (MCQST), Schellingstraße 4, 80799 München, Germany*
[6]*Philippe Meyer Institute, Physics Department, École Normale Supérieure (ENS), Université PSL, 24 rue Lhomond, F-75231 Paris, France*

(Received 25 January 2023; revised 18 April 2023; accepted 5 June 2023; published 29 June 2023)

The Trotter-Suzuki decomposition is a promising avenue for digital quantum simulation (DQS), approximating continuous-time dynamics by discrete Trotter steps of duration τ. Recent work suggested that DQS is typically characterized by a sharp Trotter transition: when τ is increased beyond a threshold value, approximation errors become uncontrolled at large times due to the onset of quantum chaos. Here, we contrast this picture with the case of integrable DQS. We focus on a simple quench from a spin-wave state in the prototypical XXZ Heisenberg spin chain, and study its integrable Trotterized evolution as a function of τ. Because of its exact local conservation laws, the system does not heat up to infinite temperature and the late-time properties of the dynamics are captured by a discrete generalized Gibbs ensemble (dGGE). By means of exact calculations we find that, for small τ, the dGGE depends analytically on the Trotter step, implying that discretization errors remain bounded even at infinite times. Conversely, the dGGE changes abruptly at a threshold value $\tau_{\rm th}$, signaling a novel type of Trotter transition. We show that the latter can be detected locally, as it is associated with the appearance of a nonzero staggered magnetization with a subtle dependence on τ. We highlight the differences between continuous and discrete GGEs, suggesting the latter as novel interesting nonequilibrium states exclusive to digital platforms.

DOI: 10.1103/PhysRevLett.130.260401

Introduction.—The intrinsic limitations in the classical simulation of quantum many-body dynamics could be overcome using a quantum computer, adopting the logic of digital quantum simulation (DQS) [1,2]. As realized early on [3], the Trotter-Suzuki decomposition [4,5] allows one to approximate the continuous-time evolution of a target system by a sequence of elementary steps, which could be implemented as quantum "gates" acting on neighboring qubits. From the experimental point of view, DQS is at an early stage if compared to "analog" quantum simulation [6,7]. Yet, the past few years have witnessed remarkable progress in the experimental control of platforms for DQS such as trapped ions [8–11] and superconducting circuits [12–17], motivating much ongoing theoretical research on the subject.

Neglecting noise, the accuracy of DQS depends on the "Trotter step" τ, which controls the number of gates applied per time unit. While many bounds on approximation errors for the system wave function exist [3,18–22], recent work [23] focused on the dynamics of local observables, putting forward the existence of a sharp "Trotter transition"; see also [24–27]. In agreement with general results on periodically driven systems [28–32], it was found that if τ is small, the discrete and continuous dynamics remain close to one another for a time that is at least exponentially long in τ_0/τ, τ_0 being some dimensionful constant. Conversely, if τ increased beyond a threshold value, approximation errors become uncontrolled, corresponding to the onset of quantum chaos [24–26]. Such transitions were found also for integrable Hamiltonians [25], as typical Trotterizations break integrability.

Here, we contrast this generic picture with the case of "integrable" DQS, focusing on the quench dynamics [33,34] of a prototypical integrable model, the XXZ Heisenberg chain [35], and its integrable Trotterized evolution [36–38]. Because of the local conservation laws, late-time physics is captured by a generalized Gibbs ensemble (GGE) [39–41]. We call it "discrete" to distinguish it from the one arising in continuous dynamics—we will show that it displays qualitatively different features. One may ask how the properties of the discrete GGE (dGGE) depend on τ. We show that, while near the continuous-time limit such dependence is analytical, the dGGE changes abruptly at a threshold value $\tau_{\rm th}$, signaling a novel type of Trotter transition. We anticipate

 © 2023 American Physical Society

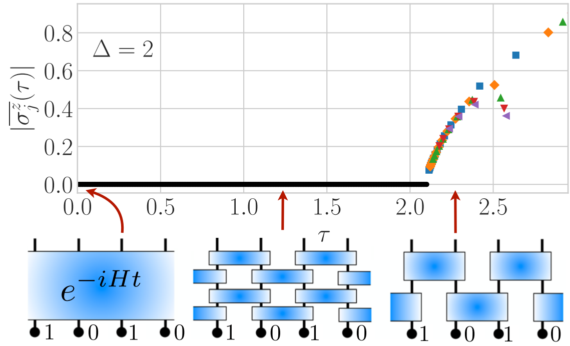

FIG. 1. Asymptotic local magnetization $|\overline{\sigma_j^z}(\tau)|$ as a function of the Trotter step τ, after a quench from the Néel state. $\overline{\sigma_j^z}(\tau)$, defined in Eq. (6), is zero for the continuous dynamics and up to a threshold value τ_{th}. For $\tau > \tau_{\text{th}}$, the dGGE changes abruptly, and the asymptotic local magnetization depends nontrivially on τ. Symbols correspond to the results of analytic computations at special values of τ (cf. the main text).

that this transition is due to a sudden change in the structure of local conservation laws, and is therefore different from traditional quantum phase transitions. Our main result is to show that this novel transition can be detected locally, as it is associated with the emergence of a nonzero staggered magnetization for quenches from a class of initial states; cf. Fig. 1. Our results highlight dGGEs as novel nonequilibrium states exclusive to DQS platforms, and could be relevant for recent experiments implementing integrable Trotterized dynamics in superconducting quantum processors [42–44].

The model.—We consider the XXZ Heisenberg model

$$H = \frac{1}{4}\sum_{j=1}^{L}[\sigma_j^x\sigma_{j+1}^x + \sigma_j^y\sigma_{j+1}^y + \Delta(\sigma_j^z\sigma_{j+1}^z - 1)], \quad (1)$$

where L is the system size, which we take to be even from now on, Δ is the anisotropy parameter, while σ_j^α are the Pauli matrices acting at position j, with $\sigma_{L+1}^\alpha = \sigma_1^\alpha$. In this Letter we focus on the gapped regime $\Delta > 1$ [35], and discuss at the end how our results depend on this choice. The Hamiltonian [Eq. (1)] is integrable, with an extensive number of local and quasilocal conservation laws [45]. As discussed earlier, the logic behind DQS is to approximate the continuous time evolution e^{-iHt} as a sequence of M unitary operators $U(t/M)$ that can be implemented via a local quantum circuit. This procedure is not unique and, in general, the discretized dynamics does not feature exact local conservation laws [25]. Here, we consider a special, yet very natural, decomposition introduced in Refs. [36,37] that preserves integrability. It is defined by the repeated application of the unitary operator $U(\tau) = U_e(\tau)U_o(\tau)$ with

$$U_o(\tau) = \prod_{n=1}^{L/2} V_{2n,2n+1}(\tau), \qquad U_e(\tau) = \prod_{n=1}^{L/2} V_{2n-1,2n}(\tau), \qquad (2)$$

and

$$V_{n,n+1}(\tau) = e^{-i\frac{\tau}{4}[\sigma_n^x\sigma_{n+1}^x + \sigma_n^y\sigma_{n+1}^y + \Delta(\sigma_n^z\sigma_{n+1}^z - \mathbb{1})]}, \qquad (3)$$

where $\tau \in \mathbb{R}$ is the Trotter step. The continuous evolution is recovered in the limit $e^{-iHt} = \lim_{M\to\infty} U(t/M)^M$.

For finite $t/M = \tau$, we a have brickwork quantum circuit (cf. Fig. 1) that can be thought of as a discrete dynamics generated by the Floquet operator $U(\tau)$. The latter is integrable: although $U(\tau)$ is not generated by a local Hamiltonian, it features an extensive number of local and quasilocal conserved operators, or "charges," that can be constructed using a standard transfer-matrix approach [36–38]. For small τ, the charges may be thought of as a deformation of those of the Eq. (1) Hamiltonian. More precisely, for each charge Q_k, with $[Q_k, H] = 0$, we have two new operators: $\tilde{Q}_k^\pm(\tau)$ with $[\tilde{Q}_k^\pm(\tau), U(\tau)] = 0$. The charges $\tilde{Q}_k^\pm(\tau)$ break the single-site translation symmetry $\mathcal{T}$, which map one onto the other, $\mathcal{T}\tilde{Q}_k^\pm(\tau)\mathcal{T}^\dagger = \tilde{Q}_k^\mp(\tau)$, whereas both $U(\tau)$ and $\tilde{Q}_k^\pm(\tau)$ are invariant under a shift of two sites, $\mathcal{T}^2$. The first pair of such charges,

$$Q_1^\pm =: \tilde{H}^\pm(\tau) = \sum_j h^\pm_{2j,2j+1,2j+2}(\tau), \qquad (4)$$

map to the Eq. (1) Hamiltonian, i.e., $\tilde{H}^\pm(\tau) \to H$ in the limit $\tau \to 0$. Here, $h^\pm_{2j,2j+1,2j+2}$ is an operator supported over three neighboring spins; cf. [46] for the exact expression.

The quench protocol.—Most existing works studying integrable Trotterizations focus on transport [36,37]. Instead, here we are interested in the quench dynamics from simple initial states for which linear response theory does not apply (see also [38,55]). It is natural to consider states respecting the two-site translation symmetry of the brickwork circuit $U(\tau)$. Specifically, here we consider a quench from the Néel state

$$|\Psi_0\rangle = |0_1\rangle \otimes |1\rangle_2 \otimes \cdots \otimes |0\rangle_{L-1} \otimes |1\rangle_L, \qquad (5)$$

where $|0\rangle_x$, $|1\rangle_x$ are the basis elements of the space at position x. Importantly, this state breaks both translation symmetry $\mathcal{T}$ and spin-flip symmetry $\mathcal{S}$ but is invariant under their joint action. As discussed later, this is the *key ingredient* for the occurrence of the transition: the latter occurs for all initial states with the same symmetry properties under $\mathcal{T}$ and $\mathcal{S}$.

We will be interested in the thermodynamic limit, and focus on local observables at late times after the quench, namely,

$$\overline{\mathcal{O}}_x(\tau) := \lim_{t\to\infty}\lim_{L\to\infty} \langle\Psi_0|[U^\dagger(\tau)]^{t/\tau}\mathcal{O}_x U(\tau)^{t/\tau}|\Psi_0\rangle, \quad (6)$$

where $\mathcal{O}_x$ is an operator with support at position x. Quantum quenches in the model [Eq. (1)] have been studied extensively in the continuous-time limit. It is known that the expectation values [Eq. (6)] are captured by a GGE [39,40], generalizing the thermal Gibbs density matrix: it is the ensemble maximizing the entropy such that expectation values of the charges match those in the initial state. This construction straightforwardly extends to the discrete dynamics [Eq. (2)] and defines the dGGE. Obtaining a quantitative description of the GGE is a notoriously difficult problem [56], which has been solved only in some cases for continuous-time evolution. As our first main result, we will generalize the tools developed in theory of quantum quenches in integrable models [41,56–58] and provide an analytic description of the dGGE for the Néel state [Eq. (5)] (as explained later, our techniques apply to a broader class of initial states). Before proceeding, we recall some basic facts about the Floquet operator [Eq. (2)].

The quasiparticle picture.—The spectrum of the Floquet operator $U(\tau)$ can be found analytically via the Bethe ansatz [59–61]. Here, we present the aspects that are directly relevant for us, and refer to Refs. [46,59] for more detail. Introducing the parameters [37]

$$\gamma = \arccos\,[\sin(\Delta\tau/2)/\sin(\tau/2)], \tag{7a}$$

$$x = i\,\mathrm{arcsinh}[\sin(\gamma)\tan(\tau/2)], \tag{7b}$$

there are two cases. First, if $\gamma = i\eta$, with $\eta \in \mathbb{R}$, then $x \in \mathbb{R}$ and $\tilde{H}^{\pm}(\tau)$ in Eq. (4) are gapped. Conversely, if $\gamma \in \mathbb{R}$, then x is purely imaginary, and $\tilde{H}^{\pm}(\tau)$ are gapless. We will refer to these cases as gapped and gapless, respectively, although we stress that $\tilde{H}^{\pm}(\tau)$ does not generate the dynamics, i.e., $U(\tau) \neq e^{-i\tau\tilde{H}^{\pm}(\tau)}$. The spectrum of $U(\tau)$ is organized into sectors labeled by the number of "magnons" M—namely, M is the quantum number associated with the conserved operator $\hat{M} = \sum_j(\mathbb{1} - \sigma_j^z)/2$. The eigenstates are parametrized by sets of complex numbers $\{p_j\}_{j=1}^M$, satisfying the quantization conditions [59]

$$\left[\frac{f_x^+(p_i)}{f_x^-(p_i)}\right]^{\frac{L}{2}} = \prod_{k\neq j}^{m} \frac{\sinh\,(p_j - p_k + i\gamma)}{\sinh\,(p_j - p_k - i\gamma)}, \tag{8}$$

where $f_x^{\pm}(p) = \sinh[p + i(x/2) \pm i(\gamma/2)]\sinh[p - i(x/2) \pm i(\gamma/2)]$. Physically, p_j are related to the quasimomenta λ_j, or "rapidities," of the quasiparticles: we have $\lambda_j = p_j \in \mathbb{R}$ and $\lambda_j = ip_j \in [-\pi/2, \pi/2]$ in the gapless and gapped regimes, respectively. When $x = 0$, Eq. (8) coincides with the standard Bethe equations for the model [Eq. (1)]. In this case, we have a simplification in the thermodynamic limit $L, M \to \infty$, with the density $D = M/L$ kept fixed: the string hypothesis [62] states that the rapidities organize themselves into sets of n elements forming a "string," which is interpreted as a bound state of n quasiparticles. Each one is associated with a string center λ, corresponding to the bound-state quasimomentum. Accordingly, macrostates are described by the functions $\rho_n(\lambda)$: in a large volume L, $L\rho_n(\lambda)d\lambda$ yields the number of n-quasiparticle bound states with rapidities in the interval $[\lambda, \lambda + d\lambda]$ [62]. Analogously to the case of free quantum gases, one also introduces the distribution function $\rho_n^h(\lambda)$ for the quasiparticles' "holes," i.e., the allowed values of the rapidities that are not occupied [62]. In the following, we will assume that the string hypothesis also holds for $x \neq 0$, extending this thermodynamic description to the discrete dynamics [63].

The dGGE.—In order to provide a quantitative description of the dGGE, we compute exactly the corresponding set of functions $\rho_n(\lambda)$ and $\rho_n^h(\lambda)$. This is a hard problem that, in the continuous-time limit, was first solved in Refs. [64–67] via the so-called quench-action approach [56,68]. Here, we follow a different strategy, developed in Refs. [58,69–71], that can be applied analytically for certain classes of "integrable" initial states [58,72]. It is based on the study of the so-called quantum transfer matrix, generating a suitably defined space-time rotated dynamics [58,73]. This approach can be naturally extended to the setting of discrete dynamics consisted here. This step, however, is technical and we report it in the Supplemental Material [46]; see also [74]. Here, we simply present the final result of our analysis.

The structure of the solution depends on the value of γ. For definiteness, let us consider the gapped regime $\gamma = i\eta$, with $\eta \in \mathbb{R}$, which holds for small τ. Introducing the standard notation [62] $\eta_n(\lambda) = \rho_n^h(\lambda)/\rho_n(\lambda)$, we derive the following analytic expression for the dGGE:

$$\eta_1(\lambda) = -1 + [1 + \mathfrak{a}(\lambda - i\eta/2)][1 + 1/\mathfrak{a}(\lambda + i\eta/2)], \tag{9}$$

where

$$\mathfrak{a}(\lambda) = \frac{\sin(2\lambda + i\eta)}{\sin(2\lambda - i\eta)} \frac{\sin(\lambda - x/2 - i\eta)}{\sin(\lambda + x/2 + i\eta)} \frac{\sin(\lambda - x/2)}{\sin(\lambda + x/2)}, \tag{10}$$

while $\eta_n(\lambda)$ for $n > 1$ are defined by

$$\eta_{n+1}(\lambda) = -1 + \frac{\eta_n(\lambda + i\eta/2)\eta_n(\lambda - i\eta/2)}{1 + \eta_{n-1}(\lambda)} \tag{11}$$

with $\eta_0(\lambda) \equiv 0$. Equations (9)–(11) are our first main results.

For a given solution $\eta_n(\lambda)$ of the above equations, one can obtain the functions $\rho_n(\lambda)$ via the following integral equations:

$$\rho_n(\lambda)[1 + \eta_n(\lambda)] = a_n^{(x/2)}(\lambda) - \sum_{m=1}^{\infty} (a_{nm} * \rho_m)(\lambda), \tag{12}$$

which are obtained from the thermodynamic limit of Eq. (8) [46]. Here, $(f * g)(\lambda) := \int_{-\pi/2}^{\pi/2} d\mu f(\mu - \lambda)g(\mu)$,

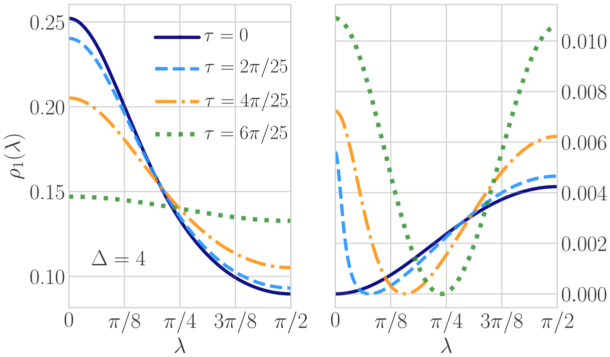

FIG. 2. dGGE quasiparticle distribution functions $\rho_n(\lambda)$ for $n = 1$, 2 and different values of τ in the gapped phase. The functions are symmetric with respect to $\lambda = 0$, and the plot only shows the region $[0, \pi/2]$.

while we introduced the notation $f^{(x)}(\lambda) = [f(\lambda + x) + f(\lambda - x)]/2$, and defined

$$a_{nm}(\lambda) = (1 - \delta_{nm})a_{|n-m|}(\lambda) + 2a_{|n-m|+2}(\lambda) + \cdots + 2a_{n+m-2}(\lambda) + a_{n+m}(\lambda), \tag{13}$$

with $a_n(\lambda) = \pi^{-1}\sinh(n\eta)/[\cosh(n\eta) - \cos(2\lambda)]$. Equation (12) can be solved numerically by standard iterative approaches [62]. An example of the solution is reported in Fig. 2 for different values of τ.

Similar analytic solutions can be obtained from any of the integrable states of the XXZ Hamiltonian [58]. These include, among others, all product states $|\Psi_0\rangle = |\psi\rangle^{\otimes L/2}$, where $= |\psi\rangle$ is an arbitrary two-qubit state. The derivation is nontrivial, and will be reported elsewhere [74].

The Trotter transition.—Equations (9)–(11) describe the dGGE in the gapped phase, corresponding to $\Delta > 1$ and small τ. When the Trotter step is increased beyond the threshold value

$$\tau_{\rm th}(\Delta) = \frac{2\pi}{\Delta + 1}, \tag{14}$$

the system enters the gapless regime, and the solution for γ in Eq. (7a) becomes real. [75]. This phase persists up to $\tau = 2\pi/\Delta$, after which further phase transitions appear [46]. We will restrict our work to this first gapless phase, but similar analyses can be carried out in the other cases.

The structure of the quasiparticle spectrum in the gapless regime is complicated [59]. Similarly to the Hamiltonian case [62], however, simplifications occur at the special points $\gamma/\pi \in \mathbb{Q}$ known as roots of unity. In this case, the string hypothesis still holds, but there are a finite number $N_b < \infty$ of bound-state types. They are described by the distribution functions $\{\rho_n(\lambda)\}_{n=1}^{N_b}$, with $\lambda \in (-\infty, \infty)$, satisfying a suitable modification of Eq. (8) [46]. For these values of γ, we are able to extend our results [Eqs. (9)–(11)], and obtain the distribution functions $\rho_n(\lambda)$ corresponding to the dGGE [46].

The quasiparticle description of the dGGE thus changes abruptly for $\tau > \tau_{\rm th}(\Delta)$. An important question, however, is whether this transition is visible in the correlation functions. One can expect this to be the case because the distribution functions $\rho_n(\lambda)$ completely specify the expectation values of local operators [76–79]. In order to identify which observables could detect the transition, we leverage the results of Refs. [36,37], studying the structure of conservation laws for the discrete dynamics [Eq. (2)]. There, it was found that at the root-of-unity points the system displays additional conservation laws breaking the spin-flip symmetry. This suggests that the transition should be visible in the late-time limit $\overline{\sigma_j^z}(\tau)$, as defined in Eq. (6).

Because of the symmetries of the initial state, $\overline{\sigma_{2j}^z}(\tau) = -\overline{\sigma_{2j+1}^z}(\tau)$, so that $\overline{\sigma_j^z}(\tau)$ coincides with the intensive value of the staggered magnetization. In order to compute it, we exploit the microcanonical interpretation of the dGGE [68], in which $\rho_n(\lambda)$ are seen as the rapidity distribution functions of a typical eigenstate in the ensemble. Considering the known finite-size formula for the expectation value of σ_{2k}^z in an eigenstate of a suitable XXZ transfer matrix with arbitrary inhomogeneities [80,81], and specializing it to our case, we find [46]

$$\langle\{\lambda_j\}|\sigma_{2k}^z|\{\lambda_j\}\rangle = 1 + 2w^T G^{-1} v. \tag{15}$$

Here, $|\{\lambda_j\}\rangle$ is a normalized eigenstate of the Floquet operator $U(\tau)$ and we introduced the Gaudin matrix $G_{ij} = L\delta_{ij}[a_2^{(x/2)}(\lambda_i) - \sum_k a_2(\lambda_i - \lambda_j)/L] + a_2(\lambda_i - \lambda_j)$ together with the two vectors $w_i = 1$ and $v_i = -a_2(\lambda_i - x/2)$. The expectation value of σ_{2k}^z in the dGGE is finally obtained by taking the thermodynamic limit of Eq. (15), assuming that the rapidities distribute according to $\rho_n(\lambda)$. In the gapped regime, this yields [46]

$$\overline{\sigma_j^z}(\tau) = 1 - 2\sum_{n=1}^{\infty} n \int_{-\pi/2}^{\pi/2} d\lambda [1 + \eta_n(\lambda)]^{-1} b_n^{\rm eff}(\lambda), \tag{16}$$

where we defined $b_n^{\rm eff}(\lambda)$ as the solution to the equation $b_n^{\rm eff}(\lambda) = b_n(\lambda) - \sum_m [a_{nm} * (1 + \eta_m)^{-1} b_m^{\rm eff}](\lambda)$, while $b_n(\lambda) = a_n(\lambda - x/2)$. An analogous expression can be derived in the gapless regime for root-of-unity points [46].

Plugging the exact rapidity distribution functions of the dGGE into Eq. (16), we obtain an analytic prediction for the asymptotic staggered magnetization. For $\tau < \tau_{\rm th}(\Delta)$, we find $\overline{\sigma_j^z}(\tau) \equiv 0$. We note that, in the continuous-time limit, this simply follows from the fact that the initial state has zero magnetization and from the late-time restoration of translation symmetry [82]. For $\tau > \tau_{\rm th}(\Delta)$, we find $\overline{\sigma_j^z}(\tau) \neq 0$. An example of our data is reported in Fig. 1, showing a clear transition at $\tau_{\rm th}(\Delta)$. We have tested our predictions against infinite time-evolving block decimation numerical calculations [46,83], as reported in Fig. 3. The

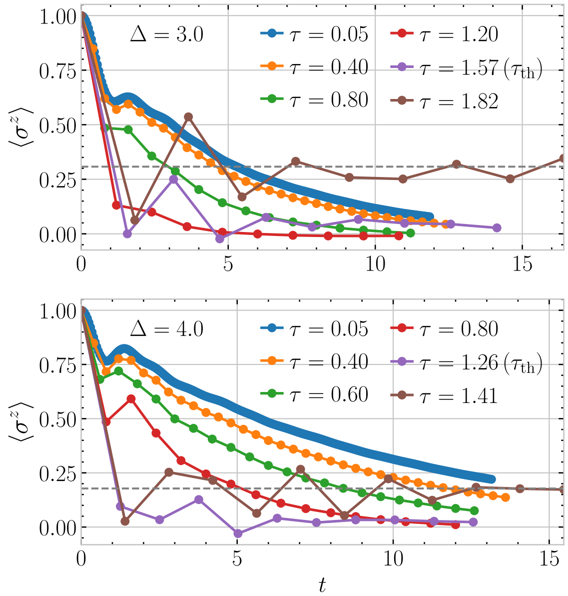

FIG. 3. Time evolution of the staggered magnetization. The plots are consistent with a vanishing value of $\overline{\sigma_j^z}(\tau)$ for $\tau < \tau_{\rm th}(\Delta)$. We also plot the dynamics for one value of $\tau > \tau_{\rm th}(\Delta)$, corresponding to $\gamma = \pi/3$ (brown lines). We see very good agreement with our analytic prediction [Eq. (16)] (dashed lines).

plots are consistent with a vanishing value of $\overline{\sigma_j^z}(\tau)$ for $\tau < \tau_{\rm th}(\Delta)$, while they show very good agreement with our analytic result at the values of τ corresponding to root-of-unity points. These quantitative predictions for $\overline{\sigma_j^z}(\tau)$ are the second main result of our work.

Since we only study rational γ/π, we cannot provide predictions for all $\tau > \tau_{\rm th}(\Delta)$. In practice, the numerical evaluation of $\overline{\sigma_j^z}(\tau)$ in the gapless phase becomes harder as the number of strings N_b increases. This is why we report only a finite number of points in Fig. 1. In general, it appears that $\overline{\sigma_j^z}(\tau) \to 0$ in a nonanalytic way as $\tau \to \tau_{\rm th}(\Delta)$. In fact, our data may be consistent with a nowhere continuous dependence of $\overline{\sigma_j^z}(\tau)$ on τ. This behavior would be analogous to that of the so-called Drude weight [84,85] characterizing transport in the gapless XXZ chain, both in the continuous- [86–88] and discrete-time setting [37]. We leave the study of the full dependence of $\overline{\sigma_j^z}(\tau)$ on τ as an interesting open question.

Our predictions were derived for the Néel state, but, as anticipated before, they hold far more generally. Indeed, the underlying mechanism for the transition is a sudden change in the structure of the conserved charges: for $\tau > \tau_{\rm th}(\tau)$ additional charges breaking spin-flip symmetry appear. This immediately implies that all the states with the same properties of the Néel state with respect to one-site shift and spin-flip symmetry show the same phenomenology [46]. Namely, any quench from an initial state $|\Psi_0\rangle$ breaking $\mathcal{T}$ and $\mathcal{S}$ individually, but preserving the combined symmetry $\mathcal{T}\mathcal{S}$, displays a discontinuous behavior in the staggered magnetization.

Finally, we comment on the dependence of our results on the choice $\Delta > 1$. It is easy to see that for $0 < \Delta < 1$, a transition still takes place at the Trotter step [Eq. (14)], but $\overline{\sigma_j^z}(\tau)$ is identically zero above $\tau_{\rm th}(\Delta)$, rather then below it. The points $\Delta = 0$ and $\Delta = 1$ are special, since in this case the system remains in the gapless regime for all τ. For $\Delta = 0$ the dynamics maps to free fermions, and can be studied exactly, as we show in the Supplemental Material [46]. Conversely, the case $\Delta = 1$ requires a dedicated analysis, which we leave for future research [74].

Outlook.—Our work opens several directions. First, our quasiparticle description of the dGGE lays the basis to study entanglement dynamics at large space-time scales, extending the results of Refs. [89,90] to the discrete setting. Similarly, it also paves the way to the application of the so-called generalized hydrodynamic theory [91,92] to integrable quantum circuits. Using these tools, it would be particularly interesting to understand how the Trotter transitions studied here affect the coarse-grained dynamics of entanglement and local observables.

We thank Pasquale Calabrese for useful discussions. B. B. was supported by the Royal Society through the University Research Fellowship No. 201101. G. G. acknowledges support from the Deutsche Forschungsgemeinschaft (DFG, German Research Foundation) under Germany's Excellence Strategy—EXC-2111–390814868 and from the ERC grant QSIMCORR, ERC-2018-COG, No. 771891.

[1] R. P. Feynman, Int. J. Theor. Phys. **21**, 467 (1982).
[2] I. M. Georgescu, S. Ashhab, and F. Nori, Rev. Mod. Phys. **86**, 153 (2014).
[3] S. Lloyd, Science **273**, 1073 (1996).
[4] H. F. Trotter, Proc. Am. Math. Soc. **10**, 545 (1959).
[5] M. Suzuki, J. Math. Phys. (N.Y.) **32**, 400 (1991).
[6] J. Preskill, Quantum **2**, 79 (2018).
[7] A. J. Daley, I. Bloch, C. Kokail, S. Flannigan, N. Pearson, M. Troyer, and P. Zoller, Nature (London) **607**, 667 (2022).
[8] B. P. Lanyon, C. Hempel, D. Nigg, M. Müller, R. Gerritsma, F. Zähringer, P. Schindler, J. T. Barreiro, M. Rambach, G. Kirchmair *et al.*, Science **334**, 57 (2011).
[9] J. T. Barreiro, M. Müller, P. Schindler, D. Nigg, T. Monz, M. Chwalla, M. Hennrich, C. F. Roos, P. Zoller, and R. Blatt, Nature (London) **470**, 486 (2011).
[10] R. Blatt and C. F. Roos, Nat. Phys. **8**, 277 (2012).
[11] C. Monroe, W. C. Campbell, L.-M. Duan, Z.-X. Gong, A. V. Gorshkov, P. W. Hess, R. Islam, K. Kim, N. M. Linke, G. Pagano, P. Richerme, C. Senko, and N. Y. Yao, Rev. Mod. Phys. **93**, 025001 (2021).
[12] Y. Salathé, M. Mondal, M. Oppliger, J. Heinsoo, P. Kurpiers, A. Potočnik, A. Mezzacapo, U. Las Heras, L. Lamata, E. Solano *et al.*, Phys. Rev. X **5**, 021027 (2015).

[13] R. Barends, L. Lamata, J. Kelly, L. García-Álvarez, A. G. Fowler, A. Megrant, E. Jeffrey, T. C. White, D. Sank, J. Y. Mutus *et al.*, Nat. Commun. **6**, 1 (2015).
[14] N. K. Langford, R. Sagastizabal, M. Kounalakis, C. Dickel, A. Bruno, F. Luthi, D. J. Thoen, A. Endo, and L. DiCarlo, Nat. Commun. **8**, 1 (2017).
[15] G. Wendin, Rep. Prog. Phys. **80**, 106001 (2017).
[16] M. Kjaergaard, M. E. Schwartz, J. Braumüller, P. Krantz, J. I.-J. Wang, S. Gustavsson, and W. D. Oliver, Annu. Rev. Condens. Matter Phys. **11**, 369 (2020).
[17] S. Bravyi, O. Dial, J. M. Gambetta, D. Gil, and Z. Nazario, J. Appl. Phys. **132**, 160902 (2022).
[18] A. M. Childs, D. Maslov, Y. Nam, N. J. Ross, and Y. Su, Proc. Natl. Acad. Sci. U.S.A. **115**, 9456 (2018).
[19] A. M. Childs and Y. Su, Phys. Rev. Lett. **123**, 050503 (2019).
[20] M. C. Tran, S.-K. Chu, Y. Su, A. M. Childs, and A. V. Gorshkov, Phys. Rev. Lett. **124**, 220502 (2020).
[21] A. M. Childs, Y. Su, M. C. Tran, N. Wiebe, and S. Zhu, Phys. Rev. X **11**, 011020 (2021).
[22] D. Layden, Phys. Rev. Lett. **128**, 210501 (2022).
[23] M. Heyl, P. Hauke, and P. Zoller, Sci. Adv. **5**, eaau8342 (2019).
[24] T. Ishii, T. Kuwahara, T. Mori, and N. Hatano, Phys. Rev. Lett. **120**, 220602 (2018).
[25] L. M. Sieberer, T. Olsacher, A. Elben, M. Heyl, P. Hauke, F. Haake, and P. Zoller, npj Quantum Inf. **5**, 1 (2019).
[26] C. Kargi, J. P. Dehollain, F. Henriques, L. M. Sieberer, T. Olsacher, P. Hauke, M. Heyl, P. Zoller, and N. K. Langford, arXiv:2110.11113.
[27] K. Chinni, M. H. Muñoz Arias, I. H. Deutsch, and P. M. Poggi, PRX Quantum **3**, 010351 (2022).
[28] D. A. Abanin, W. De Roeck, and F. Huveneers, Phys. Rev. Lett. **115**, 256803 (2015).
[29] D. A. Abanin, W. De Roeck, W. W. Ho, and F. Huveneers, Phys. Rev. B **95**, 014112 (2017).
[30] D. Abanin, W. De Roeck, W. W. Ho, and F. Huveneers, Commun. Math. Phys. **354**, 809 (2017).
[31] T. Mori, T. Kuwahara, and K. Saito, Phys. Rev. Lett. **116**, 120401 (2016).
[32] T. Kuwahara, T. Mori, and K. Saito, Ann. Phys. (Amsterdam) **367**, 96 (2016).
[33] P. Calabrese and J. Cardy, Phys. Rev. Lett. **96**, 136801 (2006).
[34] P. Calabrese and J. Cardy, J. Stat. Mech. (2007) P06008.
[35] V. E. Korepin, N. M. Bogoliubov, and A. G. Izergin, *Quantum Inverse Scattering Method and Correlation Functions* (Cambridge University Press, Cambridge, England, 1997), Vol. 3.
[36] M. Vanicat, L. Zadnik, and T. Prosen, Phys. Rev. Lett. **121**, 030606 (2018).
[37] M. Ljubotina, L. Zadnik, and T. Prosen, Phys. Rev. Lett. **122**, 150605 (2019).
[38] M. Medenjak, T. Prosen, and L. Zadnik, SciPost Phys. **9**, 003 (2020).
[39] M. Rigol, V. Dunjko, V. Yurovsky, and M. Olshanii, Phys. Rev. Lett. **98**, 050405 (2007).
[40] L. Vidmar and M. Rigol, J. Stat. Mech. (2016) 064007.
[41] F. H. Essler and M. Fagotti, J. Stat. Mech. (2016) 064002.
[42] A. Morvan, T. I. Andersen, X. Mi, C. Neill, A. Petukhov, K. Kechedzhi, D. Abanin, R. Acharya, F. Arute, K. Arya *et al.*, Nature (London) **612**, 240 (2022).
[43] K. Maruyoshi, T. Okuda, J. W. Pedersen, R. Suzuki, M. Yamazaki, and Y. Yoshida, J. Phys. A **56**, 165301 (2023).
[44] N. Keenan, N. Robertson, T. Murphy, S. Zhuk, and J. Goold, arXiv:2208.12243.
[45] E. Ilievski, M. Medenjak, T. Prosen, and L. Zadnik, J. Stat. Mech. (2016) 064008.
[46] See Supplemental Material at http://link.aps.org/supplemental/10.1103/PhysRevLett.130.260401, which includes Refs. [47–54], for further technical details.
[47] C. Destri and H. J. de Vega, Nucl. Phys. **B438**, 413 (1995).
[48] B. Bertini, P. Kos, and T. Prosen, Phys. Rev. Lett. **123**, 210601 (2019).
[49] L. Piroli, E. Vernier, P. Calabrese, and B. Pozsgay, J. Stat. Mech. (2019) 063103.
[50] L. Piroli, E. Vernier, P. Calabrese, and B. Pozsgay, J. Stat. Mech. (2019) 063104.
[51] A. Kuniba, T. Nakanishi, and J. Suzuki, J. Phys. A **44**, 103001 (2011).
[52] A. Kuniba, K. Sakai, and J. Suzuki, Nucl. Phys. **B525**, 597 (1998).
[53] R. Murgan, R. I. Nepomechie, and C. Shi, J. Stat. Mech. (2006) P08006.
[54] M. Borsi, B. Pozsgay, and L. Pristyák, J. Stat. Mech. (2021) 094001.
[55] G. Giudice, G. Giudici, M. Sonner, J. Thoenniss, A. Lerose, D. A. Abanin, and L. Piroli, Phys. Rev. Lett. **128**, 220401 (2022).
[56] J.-S. Caux, J. Stat. Mech. (2016) 064006.
[57] P. Calabrese, F. H. Essler, and G. Mussardo, J. Stat. Mech. (2016) 064001.
[58] L. Piroli, B. Pozsgay, and E. Vernier, Nucl. Phys. **B925**, 362 (2017).
[59] I. L. Aleiner, Ann. Phys. (Amsterdam) **433**, 168593 (2021).
[60] P. W. Claeys, J. Herzog-Arbeitman, and A. Lamacraft, SciPost Phys. **12**, 007 (2022).
[61] Y. Miao, V. Gritsev, and D. V. Kurlov, arXiv:2206.15142.
[62] M. Takahashi, *Thermodynamics of One-Dimensional Solvable Models* (Cambridge University Press, Cambridge, 1999).
[63] The validity of this assumption is verified *a posteriori*, based on the agreement of our predictions with numerical computations.
[64] B. Wouters, J. De Nardis, M. Brockmann, D. Fioretto, M. Rigol, and J.-S. Caux, Phys. Rev. Lett. **113**, 117202 (2014).
[65] B. Pozsgay, M. Mestyán, M. A. Werner, M. Kormos, G. Zaránd, and G. Takács, Phys. Rev. Lett. **113**, 117203 (2014).
[66] M. Brockmann, B. Wouters, D. Fioretto, J. De Nardis, R. Vlijm, and J.-S. Caux, J. Stat. Mech. (2014) P12009.
[67] M. Mestyán, B. Pozsgay, G. Takács, and M. Werner, J. Stat. Mech. (2015) P04001.
[68] J.-S. Caux and F. H. L. Essler, Phys. Rev. Lett. **110**, 257203 (2013).
[69] B. Pozsgay, J. Stat. Mech. (2013) P10028.
[70] L. Piroli, B. Pozsgay, and E. Vernier, J. Stat. Mech. (2017) 023106.
[71] L. Piroli, B. Pozsgay, and E. Vernier, Nucl. Phys. **B933**, 454 (2018).

[72] B. Pozsgay, L. Piroli, and E. Vernier, SciPost Phys. **6**, 062 (2019).

[73] A. Klümper, in *Quantum Magnetism*, Lecture Notes in Physics No. 645, edited by U. Schollwöck, J. Richter, D. J. J. Farnell, and R. F. Bishop (Springer, Berlin, Heidelberg, 2004), pp. 349–379.

[74] Bruno Bertini, Giuliano Giudici, Lorenzo Piroli, and Eric Vernier (to be published).

[75] Interestingly, for τ approaching $\tau_{\mathrm{th}}(\Delta)$ from below, the stationary state described by Eqs. (9)–(11) approaches the one of the isotropic Heisenberg chain in continuous time.

[76] M. Mestyán and B. Pozsgay, J. Stat. Mech. (2014) P09020.

[77] L. Piroli, E. Vernier, and P. Calabrese, Phys. Rev. B **94**, 054313 (2016).

[78] L. Piroli, E. Vernier, P. Calabrese, and M. Rigol, Phys. Rev. B **95**, 054308 (2017).

[79] A. Bastianello, L. Piroli, and P. Calabrese, Phys. Rev. Lett. **120**, 190601 (2018).

[80] N. Kitanine, J. Maillet, and V. Terras, Nucl. Phys. **B554**, 647 (1999).

[81] N. Kitanine, J. M. Maillet, and V. Terras, Nucl. Phys. **B567**, 554 (2000).

[82] M. Fagotti, M. Collura, F. H. L. Essler, and P. Calabrese, Phys. Rev. B **89**, 125101 (2014).

[83] U. Schollwöck, Ann. Phys. (Amsterdam) **326**, 96 (2011).

[84] V. B. Bulchandani, S. Gopalakrishnan, and E. Ilievski, J. Stat. Mech. (2021) 084001.

[85] B. Bertini, F. Heidrich-Meisner, C. Karrasch, T. Prosen, R. Steinigeweg, and M. Žnidarič, Rev. Mod. Phys. **93**, 025003 (2021).

[86] T. Prosen, Phys. Rev. Lett. **106**, 217206 (2011).

[87] T. Prosen and E. Ilievski, Phys. Rev. Lett. **111**, 057203 (2013).

[88] M. Collura, A. De Luca, and J. Viti, Phys. Rev. B **97**, 081111(R) (2018).

[89] V. Alba and P. Calabrese, Proc. Natl. Acad. Sci. U.S.A. **114**, 7947 (2017).

[90] B. Bertini, K. Klobas, V. Alba, G. Lagnese, and P. Calabrese, Phys. Rev. X **12**, 031016 (2022).

[91] B. Bertini, M. Collura, J. De Nardis, and M. Fagotti, Phys. Rev. Lett. **117**, 207201 (2016).

[92] O. A. Castro-Alvaredo, B. Doyon, and T. Yoshimura, Phys. Rev. X **6**, 041065 (2016).